RSC Advances

RSC Publishing

PAPER

View Article Online
View Journal | View Issue

Cite this: *RSC Adv.*, 2013, **3**, 21919

Rapid synthesis of gold nanostructures with cyclic and linear ketones†

William J. Peveler[a] and Ivan P. Parkin*[b]

Received 25th June 2013
Accepted 12th September 2013

DOI: 10.1039/c3ra44842h

www.rsc.org/advances

Colloidal gold nanoparticles were synthesised in aqueous solution by reaction of chloroauric acid with a range of simple aliphatic cyclic (cyclopentanone, cyclohexanone, cycloheptanone and cyclohexanedione) and linear (acetone and 3-hexanone) ketone reagents, at room temperature. The rate of reaction and particle morphology was found to be controlled by the enol content and solubility of the ketone. Cyclohexanediones produced a variety of small 20 nm particles in under 5 minutes, or larger gold nanostars, depending on the ketone isomer. Cyclopentanone was shown to produce near monodisperse 20 nm particles after 13 hours, and cycloheptanone gave polydisperse particles, but in only 50 minutes. However the linear ketones, 3-hexanone and acetone, did not produce stable colloidal suspensions. The mechanism of gold nanoparticle formation *via* reaction of ketones with chloroauric acid is discussed.

1 Introduction

Colloidal suspensions of gold nanoparticles (AuNPs) are a current focus of research within the field of nanotechnology. They have applications in bio-labelling, drug delivery, and single molecule detection, due to their small size, tuneable morphology, surface plasmon resonance (SPR) bands and ease of surface functionalisation.[1–5] AuNPs are also widely incorporated into colorimetric, fluorometric, electrochemical and Raman based sensing mechanisms for toxic and dangerous materials such as explosives, heavy metals and nerve agents.[6–8] In particular Surface Enhanced Raman Spectroscopy (SERS) has shown great potential for detection of trace amounts of these substances, with gold nanoparticles or nanostars as the enhancement agent.[9–11]

The most common synthetic routes for production of gold colloid are the Turkavich/Frens and Brust syntheses.[12–15] The former employs boiling sodium citrate solution and the latter sodium borohydride with organic solvents. Other methods of initiation are also possible.[16] Other morphologies have been formed, such as nanostars, by use of pre-formed Au seed particles.[5,17] In 2004 the first demonstration of controlled formation of AuNPs by β-diketones was presented.[18]

Recently attention has been focussed on so called 'green' syntheses of nanoparticles and large gold nanoplates, using low temperatures and natural plant extracts in water. These have been posited to proceed *via* various reduction mechanisms, but often highlight the importance of ketone groups and amides contained in the extracts, for both the reduction and stabilisation of the particle surface.[19–25] However it is rarely clear which components in the biological extracts are responsible for reduction, or present on the surface – making further surface modification potentially difficult.

In order to explore this reduction mechanism further, and extend the knowledge base from diketones to include monoketones, a new room temperature synthesis of colloidal AuNPs was recently demonstrated by Uppal *et al.*[18,26] They described a self-initiating, room-temperature synthesis of polydisperse, *ca.* 40 nm gold colloid with cyclohexanone in water. The ketone acted as both reducing agent and provided particle surface stabilisation. Most importantly they postulated a mechanism for the reduction of Au^{3+} to Au^{1+} following the chlorination of the α-position to the ketone and disproportionation of the Au^{1+} salt to give Au nanoparticles, as with the standard citrate mechanism.[27] This is a plausible demonstration of the reduction mechanism occurring during the 'green' syntheses with ketone containing plant extracts as well as the previous work with diketones, and over time produced similar, large triangular plates as observed in the various green syntheses.[18,20]

In order to further probe the mechanism at work, and investigate practical synthesis of AuNPs using simple binary mixtures at room temperature, we report here an investigation of five cyclic ketones, including two diketones, and two examples of linear ketones. A combination of analysis techniques and experimental design have provided more evidence for the reaction mechanism described, along with information on how careful choice of ketone can control the production of monodisperse AuNPs with easily modifiable surface functionalisation, for practical application.

[a]*Dept. of Security and Crime Science, University College London, 35 Tavistock Sq., London, WC1H 9EZ, UK*

[b]*Dept. of Chemistry, University College London, 20 Gordon St., London, WC1H 0AJ, UK. E-mail: i.p.parkin@ucl.ac.uk; Fax: +44 (0)20 7679 7463; Tel: +44 (0)20 7679 4669*

† Electronic supplementary information (ESI) available: Additional absorption spectra, XPS spectra, further TEM analysis and NMR data. See DOI: 10.1039/c3ra44842h

2 Experimental

Reagents were used as supplied from Sigma Aldrich, without further purification. All water used was deionised (>15 MΩ), and reactions were performed at room temperature (*ca.* 20 °C).

UV-Visible (UV-Vis) spectroscopy was performed with a Perkin-Elmer Lamda-25 instrument. ^{1}H NMR spectra were collected at 600 MHz on a Brucker AV600 spectrometer, fitted with a cryoprobe, in D_2O. Where necessary, solvent suppression was used during data collection. TEM samples were prepared by dropping 2 or 3 drops of undiluted suspension onto carbon-coated copper grids and drying in air overnight. TEM micrographs were collected using a Jeol 1010 microscope, fitted with a Gatan Orius digital camera at a beam acceleration of 80–100 keV. Images processing and particle counting were performed with Gatan Digital Micrograph and ImageJ software. X-ray Photoelectron Spectroscopy (XPS) measurements were performed with a Thermo monochromated aluminium k-alfa photoelectron spectrometer, using monochromic Al-Kα radiation. Data was analysed with CasaXPS software.

An aqueous chloroauric acid ($HAuCl_4$) stock solution was made up to 6 mM with anhydrous $HAuCl_4$ (102 mg, 0.3 mmol) in 50 ml water. The colloidal suspensions were synthesised by mixing an excess of ketone: cyclohexanone (0.5 ml, 4.8 mmol); cyclopentanone (0.5 ml, 5.7 mmol); cycloheptanone (0.5 ml, 4.2 mmol); 1,4-cyclohexanedione (0.5 g, 4.4 mmol); 1,3-cyclohexanedione (0.5 g, 4.4 mmol); 3-hexanone (0.5 ml, 4.1 mmol) or acetone (0.5 ml, 6.8 mmol) with water (9.5 ml) in clean glass vials. Where a biphasic suspension was formed, the mixture was emulsified with vigorous shaking for a minute. $HAuCl_4$ stock solution (0.44 ml, 2.6 μmol) was then rapidly injected and the vial shaken by hand. A developing pink to purple/orange colour indicated the formation of gold colloid.

After 24 hours, portions of each reaction were freeze dried for 120 hours and submitted for XPS on carbon tape.

The reaction was scalable, and performed on a 1/10 scale with water (0.95 ml) and $HAuCl_4$ stock solution (0.04 ml, 0.26 μmol), and either cyclohexanone (0.05 ml, 0.48 mmol) or 2,2,6,6-tetramethyl-cyclohexanone (0.07 ml, 0.45 mmol). It was also repeated at various scales under nitrogen, with solvents having been degassed by bubbling with N_2 for an hour. Methanolic mixtures were made with 0.22 ml of a stock 12.7 mM $HAuCl_4$ solution, in 9.5 ml of MeOH. Cyclohexanone or cyclopentanone (0.5 ml) was then added and dissolved in the MeOH.

3 Results

Cyclohexanone has been previously shown to react with chloroauric acid ($HAuCl_4$) at room temperature in a self initiating reaction, to produce gold nanoparticles (AuNPs) of average dimension *ca.* 40 nm. The reaction initiated after around 10 minutes and went to completion within 2 hours.[26] A logical extension was to explore the reactions of other simple, cyclic ketones, namely cyclopentanone and cycloheptanone. A more complex diketone motif was then explored.

3.1 Cyclopentanone

A solution of cyclopentanone in water was made up in a clean vial, and a solution of $HAuCl_4$ was rapidly injected. The ketone was kept in massive excess (>1500 fold). After standing for around 1.5 hours, the darkening of the solution to a purple/orange colour indicated the production of AuNPs. The reaction continued to darken for a further 5 hours (Fig. 1a).

The reaction was initially followed by UV-Vis spectroscopy. A baseline was taken on a sample of water and ketone, and $HAuCl_4$ was then injected as the first scan was started. Spectra were taken at 15 minute intervals, and a similar reaction profile to that of cyclohexanone was obtained. However, that the reaction took around 75 minutes to initiate and 13 to 14 hours to go to completion (for the SPR band to stabilise at one wavelength) (Fig. 2a).

The progress of the reaction was monitored by measuring the changes in SPR band size and position as the nanoparticles grew. An SPR band became apparent at 527 nm from around 90 minutes. This continued to grow for 12 hours. As the absorption increases there is also a slight variance in the SPR band position, due to the change in dispersity following nucleation and particle growth. Initially the SPR band moves up and down between 564 and 537 nm, before slowly increasing from 400 minutes to its stable position at 570 nm. This remains constant as the SPR growth flattens off at 13 hours (Fig. 2b).

Aliquots of the solution were taken as the reaction progressed and deposited and dried on TEM grids for analysis. Aliquots were removed at 10 minutes, 30 minutes and 1, 1.5, 2, 3, 4 and 24 hours. As the reaction progressed, initially 50–100 nm diameter clumps of *ca.* 5 nm particles are visible – so called *nano-pom-poms*, which separate into normal spheroid-like particles by completion. The dispersity of the sample also apparently reduces as the reaction progresses. TEM images show that after emergence of the nano-pom-poms from 10 minutes into the reaction, separation into 10–30 nm sized particles occurs over time. These then undergo an Ostwald like ripening process to complete at the largely monodisperse (*ca.* 20 nm) colloid after 13 hours (Table 1 and Fig. 3).

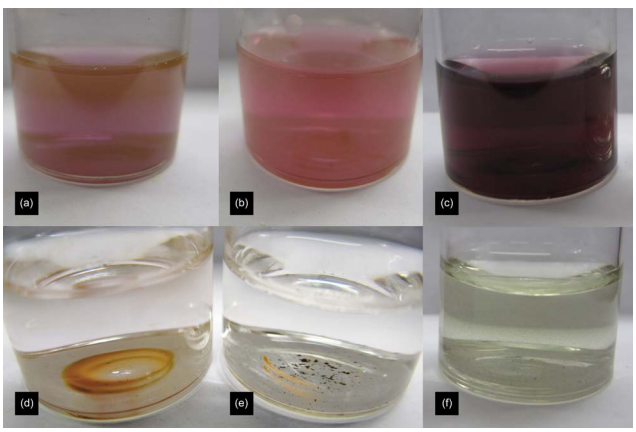

Fig. 1 Images of 24 h old nanoparticles/precipitates synthesised with (a) cyclopentanone, (b) cycloheptanone, (c) 3-hexanone, (d) acetone, (e) 1,4-cyclohexanedione and (f) 1,3-cyclohexanedione.

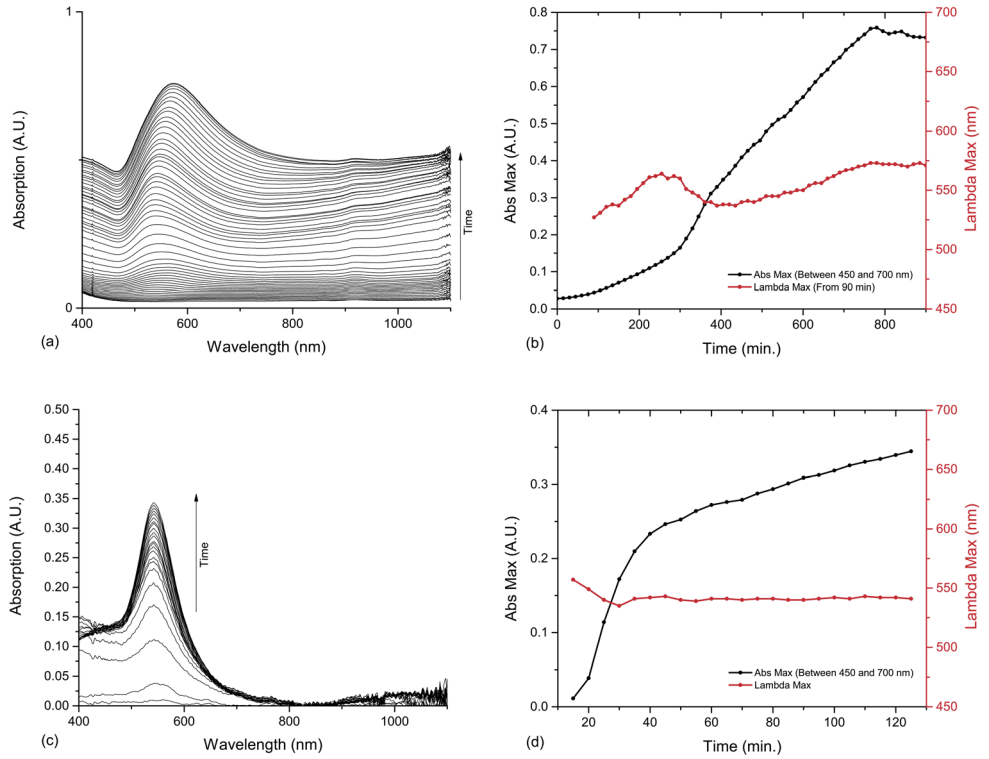

Fig. 2 UV-Vis spectroscopy and analysis of the reactions between $HAuCl_4$ and cyclopentanone and cycloheptanone. (a) UV-Vis absorption of cyclopentanone AuNPs between 0 and 810 minutes, at 15 minute intervals. (b) Development of SPR band in UV-Vis spectrum of cyclopentanone AuNPs. Maximum absorption (Abs Max) is measured between 450 and 700 nm, and the position of the SPR band maximum from its appearance at 90 minutes. (c) UV-Vis absorption of cycloheptanone AuNPs, with baseline corrected to zero at 850 nm, and data smoothed with moving average. These modifications remove the natural increase in baseline observed but correct for the inhomogeneity of the solution. (d) Development of SPR band in UV-Vis spectrum of cycloheptanone AuNPs. Abs Max is measured between 450 and 700 nm. Data plotted from 15 minutes.

In addition to the particles, a few plate like structures were also formed, predominantly triangles or truncated triangles, with side length of up to 200 nm. The prevalence of these larger shapes increased as the sample aged, with a 3 month-old sample showing predominantly thin triangular plates, of side length between 200 and 500 nm. The average size of the remaining particles also increased dramatically by TEM, as shown in Table 1, and monodispersity is lost (Fig. 3f). However UV-Vis measurements show a *ca.* 10 nm shift in the SPR band to shorter wavelengths, and a corresponding drop in absorption (see ESI†). This suggests that the larger particles may start to precipitate out.

A reaction of cyclopentanone and dilute chloroauric acid in the same ratios was repeated under oxygen-free conditions, and the reaction proceeded as above, on the same timescale. The reaction was again repeated but this time with cyclopentanone fully solubilized in methanol, and a methanolic solution of $HAuCl_4$. In this instance no evidence of reaction could be detected after several weeks.

Table 1 TEM particle counting for a sample of cyclopentanone, the same sample after three months, cycloheptanone, TMC (2,2,6,6-tetramethylcyclohexanone), 1,4-cyclohexanedione and 3-hexanone. No spherical particles suitable for counting were produced with samples of acetone or 1,3-cyclohexanedione. The number of particles (*N*), average size (Avg.) and standard deviation from the mean are given. Non-spheroidal, plate like particles were present in all samples marked with *. Cyclohexanone data are extrapolated from Uppal *et al.*[26]

Ketone sample	*N*	Avg./nm	Std. dev.
Cyclopentanone (24 hours)*	308	21	7
Cyclopentanone (3 months)*	37	93	22
Cyclohexanone*,[26]	110	43	7
Cycloheptanone*	260	21	27
TMC	129	37	11
1,4-Cyclohexanedione	154	20	5
3-Hexanone	8	139	12

3.2 Cycloheptanone

The same procedure was attempted with cycloheptanone in water instead of cyclopentanone, and although a biphasic mixture was formed, on shaking a dark purple colour appeared within 25 minutes (Fig. 1b). After an hour, a dark purple colour remained, but a gold metallic film had also formed at the solution–air interface. This film dispersed on shaking but reformed with time. The reaction was followed by UV-Vis spectroscopy as before. The baseline was corrected to account for the inhomogeneous solution, and it was possible to follow the emergence of the SPR band, indicating that the reaction initiated at *ca.* 10 min, and completed at around 50 min. The increase in baseline absorbance which is present in

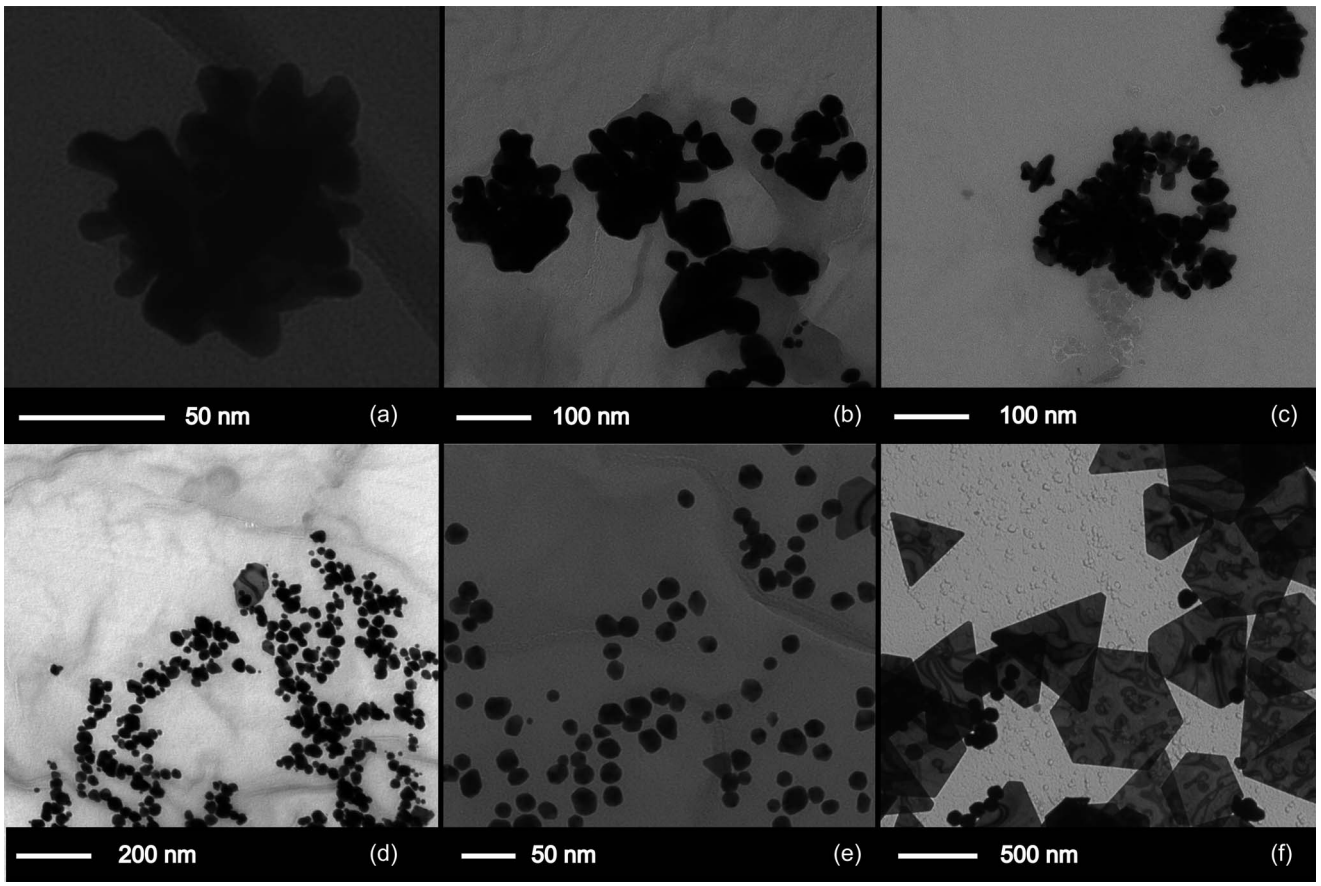

Fig. 3 TEM images of particle growth in a mixture of cyclopentanone and $HAuCl_4$. Samples were collected at (a) 10 minutes, (b) 90 minutes, (c) 180 minutes, (d) 240 minutes, (e) 24 hours and (f) 3 months.

cyclopentanone samples, is observed here, but hard to separate from the variable absorbance of the suspension, thus the spectra were baselined to ensure easier comprehension. After 50 min the SPR band continues to grow at slower but steady rate, however this may be an artefact of the cloudy solution (Fig. 2c and d).

TEM samples were taken from the cycloheptanone AuNP mixture after two and a half hours. The particles imaged were very heterogeneous, with a large range of shapes and sizes, as indicated by the large deviation in Table 1. Very large, slightly elliptical AuNPs were present, along with smaller, more conventional particles. There was also a large number of plate-like structures and some rods shapes (Fig. 4).

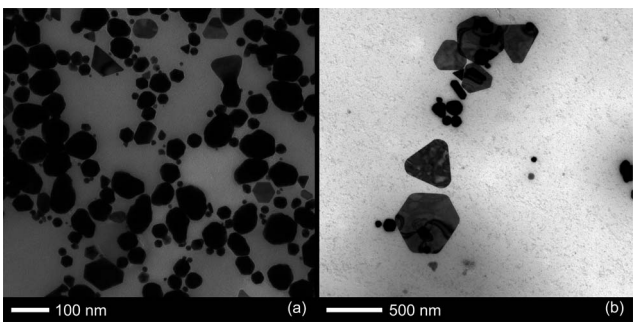

Fig. 4 TEM images of particle growth in a mixture of cycloheptanone and $HAuCl_4$. Samples were collected after around 2.5 hours of particle growth and show (a) a large variety of different particle sizes and (b) several types of thin plate.

3.3 1,4-Cyclohexanedione

A solid sample of 1,4-cyclohexanedione was dissolved in water, giving a straw-coloured solution. On injection of the $HAuCl_4$ the solution almost immediately began to darken, and after around 5 minutes had taken on a dark purple colour, shown in Fig. 1e. The reaction was followed by UV-Vis spectroscopy as before, but it proved very hard to capture the initial portion of the reaction, due to the innate time taken to perform a scan and latency in the machine. A characteristic SPR band appeared after 5 minutes, at 536 nm, and grew rapidly for 20 minutes, before plateauing. The reaction went to completion within 30 minutes (Fig. 5a and b). In contrast to the cyclopentanone reaction, there was no rise in the base line of the reaction spectra, indicating that the production of nanoparticles produced were more monodisperse.

A TEM sample was prepared from a 5 hour old sample, and the micrographs showed predominantly monodisperse, spheroidal nanoparticles, around 20 nm in diameter. There was no sign of the plates formed with cyclohexanone or

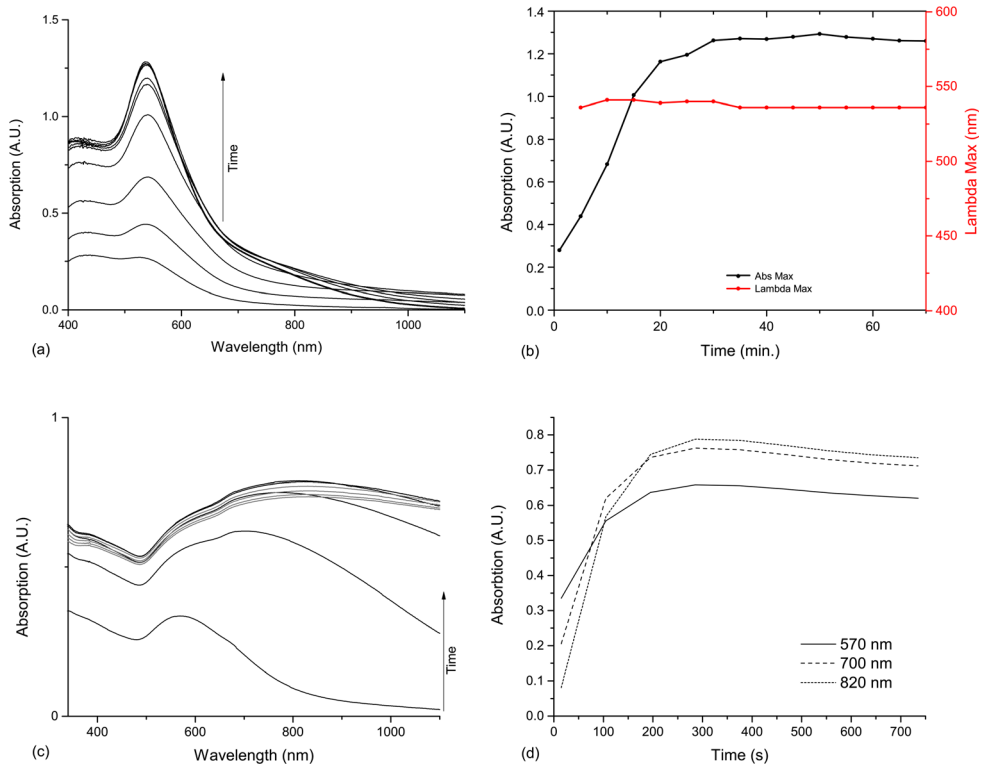

Fig. 5 UV-Vis spectroscopy and analysis of the reactions between $HAuCl_4$ and 1,4-cyclohexanedione and 1,3-cyclohexanedione. (a) UV-Vis absorption of 1,4-cyclohexanedione AuNPs between 0 and 45 minutes, at 5 minute intervals. (b) Development of SPR band in UV-Vis spectrum of 1,4-cyclohexanedione AuNPs. Maximum absorption (Abs Max) is measured between 450 and 700 nm, and the position of the SPR band maximum from its appearance at 5 minutes. (c) UV-Vis absorption of 1,3-cyclohexanedione AuNPs between increasing between 15 and 375 seconds (black) and decreasing from 375 to 735 seconds (grey) (d) Development of 570, 700 and 800 nm absorptions in UV-Vis spectrum of 1,3-cyclohexanedione AuNPs.

cyclopentanone (Fig. 6a). TEM analysis on a 4 month old sample indicated very little change in the particle morphologies or dimensions.

3.4 1,3-Cyclohexanedione

A similar reaction was performed with 1,3-cyclohexanedione, the isomer of the above diketone (Fig. 7). On injection of the $HAuCl_4$ the solution took on a blue-grey colour, again within 5 minutes. This turned slowly yellow over longer periods of time. Again the reaction was followed by UV-Vis spectrometry and similar problems were encountered in capturing the initial part of the reaction. The spectral evolution was more complex than for any of the cyclic ketones previous encountered, and is shown in Fig. 5c and d. Although in the first 60 seconds recorded, a broad SPR band grew at 570 nm, after that a larger, even broader band appeared at about 700 nm moving to 800 nm as it grew. After 6 minutes this band then started to decrease again, suggesting that the initial reaction, at least, was complete.

TEM analysis of the particles proved to be very different to all previous samples (Fig. 6b), as no conventional nanoparticles or plates were formed. Instead the sample seemed to consist almost entirely of so-called gold nanostars. These shard like structures ranged in shape and structure quite dramatically, but were roughly 200 nm in diameter.

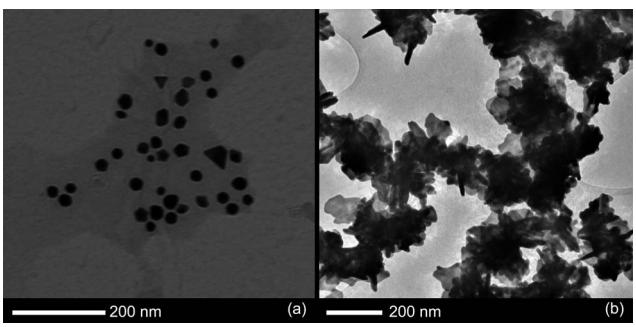

Fig. 6 TEM images of particle growth in a mixture of (a) 1,4-cyclohexanedione or (b) 1,3-cycloehexanedione and $HAuCl_4$.

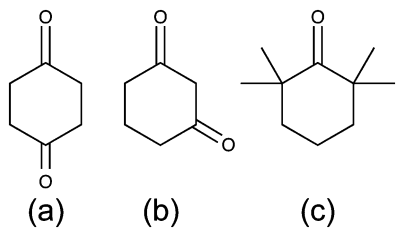

Fig. 7 Structure of (a) 1,4-cyclohexanedione, (b) 1,3-cyclohexanedione and (c) 2,2,6,6-tetramethyl-cyclohexanone (TMC).

3.5 Linear ketones

Following the success in forming AuNPs with cyclic ketones, similar reactions were attempted with two linear ketones, 3-hexanone, as a close analogue of cyclohexanone, and acetone. Acetone has been used with some degree of success before to synthesise AuNPs at elevated temperatures (boiling water), but not at room temperature.[13,28]

Reactions were set up in exactly the same way as before, but after 24 hours neither mixture showed the pink colour associated with nanoparticle formation. However the 3-hexanone mixture did have a gold sheen on the surface, similar to that occurring with cycloheptanone, and both vials showed slight traces of an orange/pink precipitate. This did not re-suspend on shaking (Fig. 1c and d).

Attempts were made to collect TEM images of the precipitate. These were unsuccessful for acetone, but a very small number of particles were imaged from the 3-hexanone vial. The measurements are summarised in Table 1.

The presence of gold was shown in all ketone samples by submitting 24 hour-old, freeze dried solutions for XPS analysis, and measurement of the 4f bands. All cyclic ketones displayed the as-expected doublet, however linear ketones also displayed a proportion of Au(III), indicating the reaction was not complete after 24 hours.†

3.6 Blocked ketones

As a test of the mechanistic theory suggested by Uppal *et al.*, a small amount of 2,2,6,6-tetramethyl-cyclohexanone (TMC – Fig. 7) was mixed with auric acid, as before. The reagents were very immiscible, but were shaken together. An identical solution containing simple cyclohexanone was also prepared concurrently.

After 30 minutes the cyclohexanone sample had started to turn a purple colour, but no change was observed for the TMC sample. After 2 hours the cyclohexanone had the typical orange/purple hue signifying the reaction was complete. The TMC had now, however, started to take a slight purple hue at the interface, signifying a limited amount of Au nanoparticle formation. NMR of the TMC showed, that although it was predominantly pure, trace amounts of unblocked ketone were also present (di and tri-methyl cyclohexanone), due to difficulty in fractional distillation of the product during synthesis, and these may have reacted with the auric acid to form the nanoparticles observed. In any case, the blocking of the α-sites significantly hindered the reaction.

4 Discussion

The reaction of ketones with chloroauric acid presents a facile method of synthesising gold nanostructures. Cyclic ketones cyclopentanone, cyclohexanone, cycloheptanone and 1,4 cyclohexanedione all produce suspensions of AuNPs of varying shapes and size. However linear ketones produce less stable particles. 1,3-Cyclohexanedione produced a solution of gold nanostar-like structures.

The original works on production of AuNPs from cyclohexanone or β-diketones posited a reaction mechanism involving the reduction of Au(III) to Au(I) *via* chlorination of the α-ketone position, disproportionation of Au(I) to produce Au(0), and stabilization of the gold nanoparticles by cyclohexanone in solution. The reaction was facilitated by the presence of the enol form of the ketone in aqueous solution, and disproportionation of Au(I) to Au(0) is catalysed on existing AuNP nuclei, giving particle growth. A suggested equivalent mechanism for reduction with cyclopentanone is given in Fig. 8. The final AuNPs are then surface stabilised by the excess ketone in solution where possible.

Following of the cyclopentanone reaction by UV-Vis spectroscopy and TEM shows how, as the Au(III) is reduced, the particle size increases with the formation and clustering of the sub 10 nm AuNP nuclei to give nano-pom-poms. These then break up and an Ostwald like ripening process occurs to even the size distribution, giving a near monodisperse colloid with of *ca.* 20 nm with an SPR band at 570 nm. After longer periods of time (months), further shape change occurs, due to the mild surface passivation by the ketone molecules. This leads to the plate growth observed, which TEM measurements indicate have a lattice spacing of around 0.235 nm. This corresponds to growth in the (111)-lattice plane.[29]

The same process seems to occur for 1,4-cyclohexanedione, but on a much more rapid timescale than anything seen before. This is likely due to the doubling of the concentration of reactive sites (two ketones per molecule) and the full water solubility of the diketones. Particle size was roughly similar to that of cyclopentanone, but with a slightly more monodisperse result. Initially no nanoplates were formed, suggesting better passivation of the particle surface.

Cycloheptanone growth was more complex, as the UV-Vis spectrum shows an relatively narrow and unmoving SPR peak at just over 540 nm, suggesting stable and monodisperse particle growth, however the TEM images are contrary to this, showing a broad mix of particle sizes. This may be linked to the poor

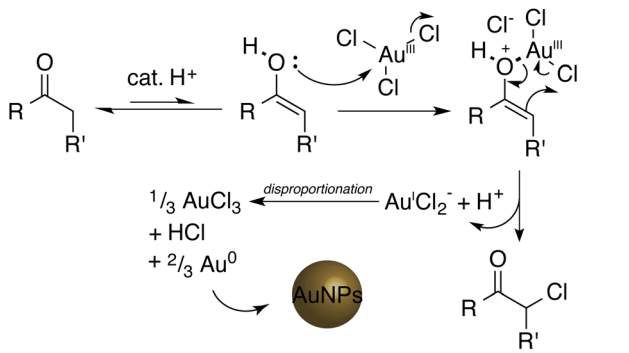

Fig. 8 Suggested reaction mechanism for the production of AuNPs with a ketone moiety and chloroauric acid. The acid catalyses tautomerism to the enol form, followed by a chloride transfer to promote reduction of Au^{3+} to Au^{+} as $AuCl_2^-$. This then undergoes a disproportionation, catalysed by any native gold present, to a mixture of Au and Au^{3+}, nucleating the gold nanoparticles. R and R′ can be connected or different (*e.g.* cyclopentanone R–R′ = $-CH_2CH_2CH_2-$, or acetone R = CH_3, R′ = H).

solubility of cycloheptanone in water, causing several different nucleation and ripening processes to occur in droplets of cycloheptanone, or at the cycloheptanone–water interface.

The second diketone, 1,3-cyclohexanedione did not produce particles or plates, but instead complex nanostar structures. This very rapid reaction suggests that the usual surface passivation mechanism does not operate, allowing parts of the crystal to grow much faster than others, creating the complex shapes observed.

Whilst cyclic ketones appear to afford mild aqueous stability for the colloid, linear ketones apparently do not. This is evidenced by the precipitation of the AuNPs in 3-hexanone, and their large size (which are interlinked). Good surface stabilisation will slow the rate of growth by passivating the surface from acting as a nucleation site, and keep the particles small and in solution.

4.1 Mechanistic testing

Several tests of the mechanism were performed by varying reaction conditions and parameters, as well as hunting for telltale byproducts.

The first, simple piece of supportive evidence was provided by the unsuccessful methanolic reaction. In the less polar solvent, it is supposed that there will be a far lower proportion of the dissociated acid, and consequently the enol that allows the chlorination to proceed, and this inhibits the reaction.

The reaction in water was tested in both the light and dark, as well as oxygenated and deoxygenated environments, and proceeds at the normal rate, thus lowering the likelihood that it is a radically or photochemically initiated process.

Finally the use of TMC as an alternative to cyclohexanone, although not completely halting particle growth due to latent impurities, slowed the growth, highlighting the importance of α-protons for enol formation.

Another way to probe if the suggested mechanism is occurring is to look for the predicted chlorinated by product in the final AuNP colloid. ^{1}H spectra were collected from repeats of the cyclopentanone, cycloheptanone, 1,3- and 1,4-cyclohexanediones, 3-hexanone and acetone reactions performed in D_2O, in an attempt to isolate the downfield shift of any peaks due to the presence of –Cl, and full NMR evidence is detailed in the ESI.†

Due to the tiny quantities of chlorinated by-product formed (less than 3.9 μmol in 10 ml) in the presence of large amounts of starting material and solvent, the signals are confined to the baseline of the spectra, and thus must be carefully separated from spectral noise and satellite peaks. There is also a close overlap of the residual water peak and any potential proton peaks. However on magnification by circa 1000 times, it was possible to see indicative proton peaks at around 4 ppm in spectra of cyclopentanone and acetone; arising from the α-halo proton. It should be noted though, that these peaks were not obvious in the more complex spectra of 3-hexanone or cycloheptanone. A more obvious change, was the unusually small integral for the α hydrogen peak of 1,3-cyclohexanedione after nanoparticle formation. These data were not in-themselves conclusive, and it proved impossible to improve the quality of the spectra. Therefore they must be treated with caution and taken into account along with all the other evidence presented here.

Finally, having shown that the enol content in methanol was too low for the reaction to proceed, it is interesting to compare the theoretical proportion of enol in aqueous solution for the sample of cyclic and linear ketones, with the characteristics of gold nanoparticles produced. Keto and enol forms of each molecule exist in dynamic equilibrium in solution, and the amount of each form is governed by a variety of factors, including molecular geometry, bond strengths and entropy effects.[30,31]

In Table 2 we compare several reaction factors, including an indication of the enol concentration (in the form of pK_E) and the solubility of the ketone; to the size and shape of any particles measured, and the rate of reaction. Enol content is expressed as $-\log_{10}\left(\frac{[\text{enol}]}{[\text{ketone}]}\right) = \text{p}K_E$ and is cited from Keeffe *et al.* or chemical handbooks.[30] The value for 3-hexanone, and 1,4-cyclohexanedione are not expressly given. Thus the values for 3-hexanone is instead approximated from 3-pentanone (7.43) and the value for 1,4-cyclohexanedione is assumed to be slightly lower than that of cyclohexanone (6.38).

We see a general trend, that as the quoted literature pK_E of the ketone increases (that is, the amount present in solution decreases) the rate of reaction tends to decrease, from 1,3-cyclohexanedione to the linear ketones (this is also supported by the XPS data†). However an anomaly does arise for cycloheptanone.

The large pK_E of cycloheptanone should indicate a low enol availability and thus slow AuNP formation, however this is not

Table 2 Summary of growth rate and morphology control exerted by various ketones related to their solubility and enol content. Enol content is expressed as pK_E and data are extracted from Keeffe *et al.*[30]

Ketone	Solubility/ mg ml^{-1}	pK_E	Reaction time	Average particle size/nm
1,3-Cyclohexanedione	Soluble	5.26	~5 min	Nanostars
1,4-Cyclohexanedione	Soluble	<6.38	30 min	20 nm
Cyclohexanone	90	6.38 (ref. 30)	1 hour	40 nm
Cyclopentanone	9	7.94 (ref. 30)	13 h	21 nm
3-Hexanone	15	~7.43	>24 h	138 nm
Cycloheptanone	<1	8.00 (ref. 30)	50 min	*ca.* 20 nm
Acetone	Miscible	8.33 (ref. 30)	>24 h	—

the case. We suggest that solution effects may also play a part. As the cycloheptanone has a low solubility, much of the reaction may take place at the surface of droplets in the emulsion formed, thus greatly increasing the local concentration of cycloheptanone, and pushing up the rate of reaction. The particles may actually become trapped in the droplets and segregate to the top of the solution, creating the gold sheen observed.

The rate of reaction for formation of AuNPs will impact the size of AuNPs formed, with slower growth rates in theory leading to larger particles, due to fewer nucleation sites accepting a larger proportion of the gold nuclei available. The very reactive 1,3-cyclohexanedione, with its very high enol content, reacts very rapidly as expected, and this may influence the odd shapes produced, rather than small particles as expected. In addition to this the shape of the molecule makes it likely to be bi-dentate, affecting how it will ligate to and stabilise the gold particles.

It is also important to note, however, that the effect of ketone solubility may also be a key factor the size, shape and dispersity of the nanoparticles produced. Higher solubility of the ketone would ensure a better-mixed solution when the $HAuCl_4$ was injected, giving faster and more homogeneous production of the initial gold seeds. This would explain the smaller, more evenly sized particles. By contrast, a very heterogeneous solution, such as in the case of cycloheptanone, would mean gold seeds would be produced at various time points throughout the reaction, in regions of localised concentration, resulting in various different growth rates, and particle sizes.

5 Conclusions

Colloidal AuNPs have been produced by room temperature, self-initiating reaction of cyclic ketones and dilute $HAuCl_4$. Reduction of Au^{3+} has also been achieved with linear ketones: acetone and 3-hexanone, but no colloidal suspension was achieved. 1,4-Cyclohexanedione gave near monodisperse 20 nm gold nanoparticles at room temperature, with the reaction initiating in seconds, and completing in minutes.

Cyclopentanone allowed the growth mode to be studied, exhibiting pom-pom formation followed by growth of spheroidal nanoparticles of *ca.* 20 nm in size. Other shapes accessed with cyclic ketones included larger particles, as well as large flat triangular and hexagonal plates. In particular gold nanostars were produced with a solution of 1,3-cyclohexanedione, giving a promising SERS enhancement agent.

Several techniques were used to probe the reaction mechanism. Lowering the available enol content, and observing a lowering of the reaction rate was achieved with a change of solvent to methanol. Blocking the reactive α-positions with methyl groups also gave a reduction in rate. NMR was used to study byproducts from the reaction.

Finally, literature enol proportions, for each ketone in water, were correlated with the rate of reaction, as followed by eye and UV-Vis spectroscopy. Generally, the lower the enol content, the slower the reaction. An exception was for cycloheptanone, where although the enol content was predicted to be lower than cyclopentanone, the reaction still proceeded rapidly. This is possibly due to the low solubility of the ketone causing concentration hotspots in the reaction mixture. It is also posited that the inhomogeneity of the solution caused the arising polydisperse nature of the nanoparticles produced.

These results add weight to the previously suggested reaction mechanism, of α-chlorination *via* an enol tautomerism of the ketone and have application in the study of so-called 'green' nanoparticle synthesis. It is clear that by using different size cyclic ketones, with variable reactivity and solubility, good control of nanoparticle morphology can be achieved.

Acknowledgements

This work was supported by EPSRC Grant no.: EP/G037264/1 as part of UCL's Security Science Doctoral Training Centre. The authors thank the UCL Institute of Opthalmology Imaging Facility for access to EM facilities and Emily Glover and Dr Rob Palgrave for assistance with XPS analysis.

References

1 C. Park, H. Youn, H. Kim, T. Noh, Y. H. Kook, E. T. Oh, H. J. Park and C. Kim, *J. Mater. Chem.*, 2009, **19**, 2310.
2 S. Guo and E. Wang, *Nano Today*, 2011, **6**, 240–264.
3 K. Saha, S. S. Agasti, C. Kim, X. Li and V. M. Rotello, *Chem. Rev.*, 2012, **112**, 2739–2779.
4 Y. Liu and A. R. H. Walker, *Angew. Chem., Int. Ed. Engl.*, 2010, **49**, 6781–6785.
5 P. Senthil Kumar, I. Pastoriza-Santos, B. Rodríguez-González, F. Javier García de Abajo and L. M. Liz-Marzan, *Nanotechnology*, 2007, **19**, 015606.
6 V. K. K. Upadhyayula, *Anal. Chim. Acta*, 2012, **715**, 1–18.
7 S. S. R. Dasary, A. K. Singh, D. Senapati, H. Yu and P. C. Ray, *J. Am. Chem. Soc.*, 2009, **131**, 13806–13812.
8 G. Aragay, J. Pons and A. Merkoçi, *Chem. Rev.*, 2011, **111**, 3433–3458.
9 R. W. Taylor, T.-C. Lee, O. A. Scherman, R. Esteban, J. Aizpurua, F. M. Huang, J. J. Baumberg and S. Mahajan, *ACS Nano*, 2011, **5**, 3878–3887.
10 J. F. Li, Y. F. Huang, Y. Ding, Z. L. Yang, S. B. Li, X. S. Zhou, F. R. Fan, W. Zhang, Z. Y. Zhou, D. Y. Wu, B. Ren, Z. L. Wang and Z. Q. Tian, *Nature*, 2010, **464**, 392–395.
11 M. P. Cecchini, *Nat. Mater.*, 2012, **11**, 1–7.
12 J. Kimling, M. Maier, B. Okenve, V. Kotaidis, H. Ballot and A. Plech, *J. Phys. Chem. B*, 2006, **110**, 15700–15707.
13 J. Turkevich, P. C. Stevenson and J. Hillier, *Discuss. Faraday Soc.*, 1951, **11**, 55–75.
14 G. Frens, *Nature*, 1973, **241**, 20–22.
15 M. Brust, M. Walker, D. Bethell, D. J. Schiffrin and R. Whyman, *J. Chem. Soc., Chem. Commun.*, 1994, 801–802.
16 M. A. Uppal, A. Kafizas, M. B. Ewing and I. P. Parkin, *New J. Chem.*, 2010, **34**, 2906.
17 A. Kedia and P. S. Kumar, *J. Mater. Chem. C*, 2013, **1**, 4540.
18 S. Kundu, A. Pal, S. K. Ghosh, S. Nath, S. Panigrahi, S. Praharaj and T. Pal, *Inorg. Chem.*, 2004, **43**, 5489–5491.

19 S. Mukherjee, V. Sushma, S. Patra, A. K. Barui, M. P. Bhadra, B. Sreedhar and C. R. Patra, *Nanotechnology*, 2012, **23**, 455103.
20 S. S. Shankar, A. Rai, B. Ankamwar, A. Singh, A. Ahmad and M. Sastry, *Nat. Mater.*, 2004, **3**, 482–488.
21 P. Dauthal and M. Mukhopadhyay, *Ind. Eng. Chem. Res.*, 2012, **51**, 13014–13020.
22 D. S. Sheny, J. Mathew and D. Philip, *Spectrochim. Acta, Part A*, 2012, **97**, 306–310.
23 D. Philip, *Spectrochim. Acta, Part A*, 2010, **77**, 807–810.
24 D. Philip, C. Unni, S. A. Aromal and V. K. Vidhu, *Spectrochim. Acta, Part A*, 2011, **78**, 899–904.
25 C. G. Kumar, S. K. Mamidyala, B. Sreedhar and B. V. S. Reddy, *Biotechnol. Prog.*, 2011, **27**, 1455–1463.
26 M. A. Uppal, A. Kafizas, M. B. Ewing and I. P. Parkin, *J. Mater. Chem. A*, 2013, **1**, 7351.
27 I. Ojea-Jiménez and J. M. Campanera, *J. Phys. Chem. C*, 2012, **116**, 23682–23691.
28 A. E. Davies, *J. Phys. Chem.*, 1929, **33**, 274–284.
29 K. Heinemann and H. Poppa, *Appl. Phys. Lett.*, 1970, **16**, 515.
30 J. R. Keeffe, A. J. Kresge and N. P. Schepp, *J. Am. Chem. Soc.*, 1990, **112**, 4862–4868.
31 A. Gero, *J. Org. Chem.*, 1961, **26**, 3156–3157.